# Use of Landsat ETM+ data for delineation of water bodies in hilly zones

Vijay S. Bhagat and Kishor R. Sonawane

## ABSTRACT

The remotely sensed Landsat Enhanced Thematic Mapper Plus (ETM+) dataset is used for the detection and delineation of water bodies in hilly zones. The water bodies were detected using Surface Wetness Index (SWI), Normalised Difference Vegetation Index (NDVI) and a slope map. The assessment of areas under dense vegetation in water bodies is omitted in the combined map prepared using classified raster images showing (1) the distribution of 'water' and 'non-water' based on SWI and (2) the distribution of 'vegetation' and 'non-vegetation' based on NDVI. The shadows' effect in estimated areas under water bodies is detected and delineated using the combination of (1) a combined raster image (classified SWI and NDVI) and (2) a slope map. About 3.8% (1370 ha) of the total area reviewed is estimated under water bodies with 91.74% overall accuracy. The water bodies include (1) major and minor dams, (2) watered streams, (3) springs distributed in foothill zones and (4) small dams on minor streams. The relatively smaller water body objects, i.e. streams and springs, have estimated less producer's (92–96%) and user's (85–92%) accuracy than the major water bodies, i.e. 96.77% producer's and 100% for user's accuracy.

**Key words** | indices slicing, map combinations, NDVI, overlay, SWI, topographic shadows

**Vijay S. Bhagat** (corresponding author)
**Kishor R. Sonawane**
Department of Geography,
Agasti Arts,
Commerce and Dadasaheb Rupwate
Science College,
Akole,
Ahmednagar 422601,
Maharashtra,
India
E-mail: *kalpvij@yahoo.co.in*

## INTRODUCTION

Over 1.2 billion people in the world do not have access to clean water to meet their basic needs and 2.6 billion do not have access to basic sanitation (WHO 2003). More than 27 nations are facing water scarcity and 19 nations are considered as water-stressed (WRI 2004). In fact, there is no real water shortage, but it is a matter of managing and distributing the resources better (Bindraban *et al.* 2006). Imbalance between availability and demand, degradation of water quality, depletion and lack of security in groundwater availability, inter-sector and intra-sector competition, and inter-regional and international conflicts are the most common water-related problems. In addition to that (1) increasing degraded and desert lands, (2) increased trend of salinisation and water logging as an impact of over-irrigation, and (3) high demand for fresh water for urban and industrial use are widely identified basic issues in water resource planning and management. These problems and issues affect applications of people–environment-focused integrated water management (Warner *et al.* 2006). It demands basic information about the quantity, quality and distribution of available water resources. Recently, leading authorities and personalities have argued the importance of information technology with public participation in the better assessment, planning and management of water resource (Troell *et al.* 2005).

The quantity, quality (Deosthali 2005; Kumar *et al.* 2007) and area covered by water bodies have been estimated by many scientists across the globe by using different ways and methods. Jongman & Padovani (2006) have noted the requirement of integration between researchers and stakeholders for water resource management in river basins.

doi: 10.2166/hydro.2010.018

Some of them have used satellite data and GIS techniques for estimations of the total volume of water in man-made as well as natural water bodies (Bhagat 2008) and pollution in water bodies including oceans, rivers, lakes and groundwater (Kumar *et al.* 2007; Pawar *et al.* 2008). The estimations include the area covered and spread of water storage and river tracks in floods and ocean water in high tide conditions in coastal areas. These techniques have become more useful in developing early flood warning systems (Mioc *et al.* 2008). Remote sensing techniques have been used to estimate water availability and productivity (Dam *et al.* 2006) with flood and drought affects on agriculture (Patel 2006).

The poorest of the poor are most affected by the lack of access to a water-based productivity system (Warner *et al.* 2006). Agriculture is a major user of the available fresh water for irrigation. Irrigation performance analyses have suggested that irrigation systems need to be rehabilitated and modernised to improve performance (Pavlov *et al.* 2006) and reach the poorest people. Agricultural water balance and the volume of irrigation water as compared to economic output and expenditure are considered as irrigation performance indicators. The available water should be used as irrigation security against the conditions of crop failure in droughts (Bhagat 2004). All these situations are suggesting the need for water volume estimations prior to applications.

Remote sensing techniques are used for estimations of water bodies by many researchers and planners in different fields, viz. hydrology, oceanography, ecology, etc. However, most of the manmade water reservoirs are located in hilly zones. Fresh water and topographic shadows appears similar in optical–infrared remote sensing data and cause confusion in the detection and delineation of water bodies in hilly zones (Small 2004). Automated delineation of shadows remains a challenging task (Racoviteanu *et al.* 2009) and visual interpretation with manual editing has been widely suggested for the correction of topographic shadowing effects. In the present study, an automated delineation technique is used to separate the water bodies and assessment of areas under topographic shadows in estimated water bodies using remote sensing data.

It is possible to assess the surface wetness by applying conventional as well as remote sensing methods. Tasselled cap transformed derivatives (TCTD) based on Landsat 4 (Crist & Cicone 1984; Crist 1985), Landsat 5 (Crist *et al.* 1986) and Landsat 7 (Huang *et al.* 2002) at-satellite reflectance are useful in estimating surface brightness, greenness, wetness, etc., for pixel to pixel DN (digital number) values. Surface Wetness Indices (SWI) based on TCTD are useful for a better understanding of the spatial distribution of surface wetness (Oza *et al.* 2006; Patel 2006; Bhagat 2009). With few limitations, the wetness indices are potentially capable of providing indications of relative variations in surface wetness conditions.

Remotely sensed data has been widely used for forest classification and their correlations with parameters like slope, soil moisture and water table (Gong *et al.* 2004; Bhagat 2009). Forest studies extensively utilize ETM+ (Landsat 7 Enhanced Thematic Mapper Plus) datasets for forest identification and classification (Gong *et al.* 2004; Ramsey *et al.* 2004) with a good accuracy level. The Normalised Difference Vegetation Index (NDVI) based on the ETM+ dataset is potentially useful to delineate whether the lands have green cover or not (Kiage *et al.* 2007).

In the present study, Landsat 7 ETM+ data is used for preparing SWI and NDVI. The SWI raster image is prepared using TCTD (Huang *et al.* 2002). Based on these images, with the help of a slope map, water bodies in hilly zones of the upper Pravara basin of the Ahmednagar district, Maharashtra (India) have been identified (Figure 1). The slope map is used for masking the area under shadows included in the estimated water bodies using SWI (Giles 2001; Bolch *et al.* 2008; Racoviteanu *et al.* 2009). Google Earth images and field verification (December 2009) were used to collect ground truth information. The methodology formulated in this study can be used as a rapid assessment tool for estimating (1) the volume of water in storage, (2) flood-affected areas, (3) water spread in tidal conditions in coastal areas and (4) waterlogged areas due to over-irrigation, mainly in hilly zones.

## STUDY AREA

The study area forms part of the upper Pravara basin (35794 ha) of the Ahmednagar district, Maharashtra (India) (Figure 1). It is a valley between two offshoots, i.e. Kulangarh-Navaricha dongar-Kalsubai (1646 m) to the north and Sipnur-Ratangarh (1237 m) to the south extended from west to east from the Sahyadri mountain (Western Ghats).

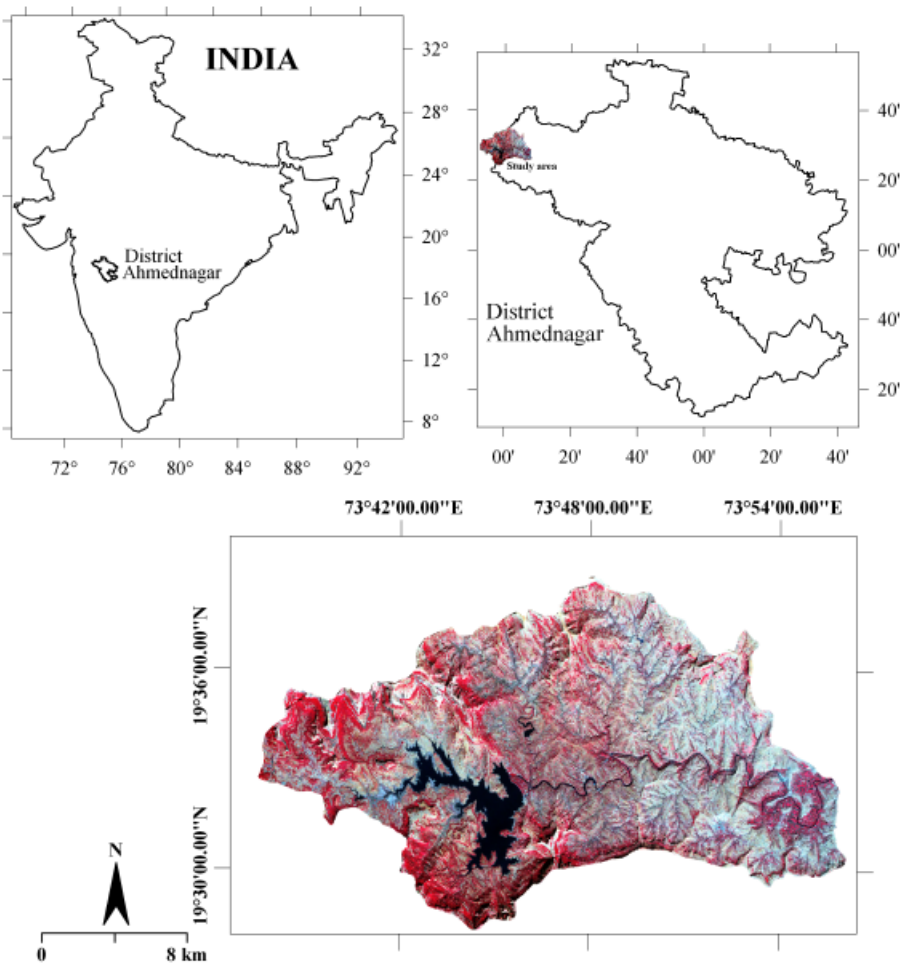


**Figure 1** | The study area: upper Pravara basin.

The slopes of these ranges are very steep, facing both north and south (Figure 2) which form shadows mainly on the northern slopes. The depth and water-holding capacity of the soils are varied according to the slopes. Downhill slopes have deep soils which sustain the wetness for a long time compared to the shallow soils. The average annual rainfall varies from 606 mm on the eastern boarder (Chitalwedhe) to 5366 mm on the western boarder (Ghatghar). The deep soils are covered by medium to dense deciduous and evergreen monsoon forests in places and also some barren land. There are three types of water bodies, i.e. (1) the major reservoir (the Wilson dam), the oldest dam (100 years) located in the central part of the study area and the Ghatghar dam in the west, (2) small dams on small tributaries in the northern area and (3) the Pravara River, the major non-perennial river flowing west to east and flooding only in the rainy season (June–September). The river sometimes has water downstream of the dam in the period given to agriculture. The Nilvande dam, located downstream from the

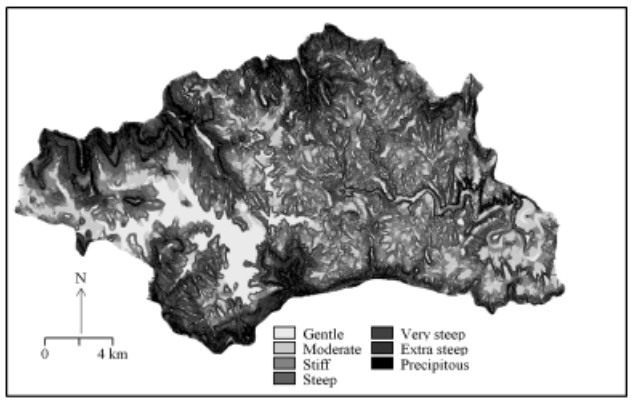


**Figure 2** | Slope categories.

Wilson dam on the Pravara River was constructed after the satellite data was captured (December 2000). This new water body is not recorded in the data used for this study.

## DATABASE AND SOFTWARE USED

The analyses for the present study are based on remotely sensed data and field checks. The rectified Landsat 7 ETM+ dataset (path 147 and row 046, December 2 2000, available at ftp://ftp.glcf.umiacs.umd.edu/) is used as it has a good accuracy of acquisition potential (Gong *et al.* 2004; Ramsey *et al.* 2004) (28.5 m pixel size, UTM (Universal Transverse Mercator) coordinates (WGS84), zone-43N) in the identification and classification of various environmental elements. This is the winter season (December) and has probably cloud-free skies in the study areas. The data is captured in cloudless weather. The surface wetness index (SWI) (Equation (1)) is estimated using bands 1–5 and 7. The Normalised Difference Vegetation Index (NDVI) (Equation (2)) is estimated using the red and infrared (IR) bands. Field checks were undertaken to verify the inferences drawn by the analyses. The remotely sensed dataset was compiled, merged and loaded into the Windows-based GIS image processing software ILWIS 3.4 Academic (2004). About 121 samples distributed in classified groups have been collected from GPS (WGS84 UTM Zone 43N)-based ground verification and Google Earth images for the assessment of accuracy.

## METHODOLOGY

Image processing (Figure 5) in the present study can be discussed in six steps: (1) preparation of FCC (False Colour Composite) (Figure 1) using bands 2–4, (2) preparation of raster image depicting surface wetness indicating wet and dry areas, (3) preparation of NDVI raster image to classify the area as vegetation or non-vegetation, (4) delineation of water bodies, (5) detection and correction of the shadows included in water bodies and (6) accuracy estimations. A simple index-slicing approach (permanent classification of raster images using fixed threshold values) is adopted for detection and delineation of water bodies (Figure 5) and a combination approach for the detection and correction of areas under non-water bodies included in the detected water bodies.

### Approach I: index slicing

#### Surface wetness index (SWI)

The spectral characteristics of water are remarkably different from other land surface types (e.g. vegetation, soil, rock, road) because of its strong absorption. Clear water has a low spectral reflectance in the visible spectral region while other surface covers have higher reflectance than water (Kiage *et al.* 2007; Hui *et al.* 2008). Water bodies can be detected and delineated using simple slicing of a single band (Hui *et al.* 2008) or raster images showing calculated indices. Frazier & Page (2000) have used band 4 (Dupigny *et al.* 1999) and band 5 using a density slicing approach for successful identification of major water bodies. The Normalized Difference Water Index (NDWI) effectively discriminates the open water from soil and vegetation (Wu *et al.* 2008). Hui *et al.* (2008) have found the NDWI and Modified Normalized Difference Water Index (MNDWI) useful for detection of changes in water bodies. The MSS (Multi Spectral Scanner) band 7 (0.8–1.1 μm) has been found particularly suitable for distinguishing water from dry surfaces due to the strong absorption of water in the near-infrared range of the spectrum (Frazier & Page 2000). Wang *et al.* (2002) have added Landsat TM band 7 to band 4 to delineate the inundated areas. Frazier & Page (2000) have found all three infrared bands performed significantly better than the visible bands for achieving high overall accuracy and user's accuracy. However, no single band can accommodate all aspects of the water environment (Ryu *et al.* 2002). The at-satellite reflectance-based Tasselled Cap Coefficients suggested by Huang *et al.* (2002) are useful to get the combined effect of bands 1–5 and 7 in a single raster image which can be sliced into different classes. The surface wetness index (Equation (1)), generated using at-satellite reflectance-based Tasselled Cap Coefficients (Huang *et al.* 2002), is tested successfully for classification of land according to different levels of surface moisture (Bhagat 2009):

$$\begin{aligned}\text{Surface Wetness Index} = ((&\text{band } 1 \times 0.2626)\\ &+ (\text{band } 2 \times 0.2141)\\ &+ (\text{band } 3 \times 0.0926)\\ &+ (\text{band } 4 \times 0.0656)\\ &+ (\text{band } 5 \times -0.7629)\\ &+ (\text{band } 7 \times -0.5388))\end{aligned} \quad (1)$$

The SWI (Equation (1)) is calculated using at-satellite-based reflectance showing maximum values for water bodies (180) and minimum values (−145) for dry lands which are rocky, sandy or barren. Values greater than 2 are considered as water and smaller values indicate no-water (Figure 3). The SWI is used to classify the reviewed area into 'water' and 'no-water' with the help of the 'slicing' operation in ILWIS. The 'slicing' operation in ILWIS is useful for permanent classification of raster images using fixed threshold values. However, the class 'water' includes areas of deep soils covered by dense 'evergreen and deciduous' forest and areas under 'topographic shadows' where SWI is comparatively larger. This added area has to be separated from the class 'water'. The validation was carried out by intensive field checks.

### Normalised difference vegetation index (NDVI)

Band 3 (red) provided a vegetation discrimination ability, as well as a heightened contrast between vegetated and non-vegetated areas (e.g. bare soil and roads). Band 4 (IR) allows the separation between water bodies and vegetation (Dupigny *et al.* 1999; Frazier & Page 2000). Therefore, the Normalized Difference Vegetation Index (NDVI) (Equation (2)) has a great potential for discrimination of the areas under water from other land cover (Sanyal & Lu 2004; Kiage *et al.* 2007). However, permanent water bodies like ocean water show a response in the visible region due to phytoplankton pigment which imparts a green colour to the sea water (Dayaker 2003). The water bodies taken into consideration for this study are temporary man-made storage areas or flowing water. They are not stable enough and suitable for growth of such kinds of plants in water:

$$\text{NDVI}=\text{IR}-\text{red}/\text{IR}+\text{red}. \quad (2)$$

The maximum NDVI (0.45) value is estimated in dense forest areas and the minimum (−0.26) in water bodies. The identified values of NDVI are broadly grouped into vegetation (>0) (deciduous and evergreen monsoon forest) and non-vegetation (<0) (water bodies, barren and rocky land) (Dupigny *et al.* 1999; Kiage *et al.* 2007) classes (Figure 4) with the help of the 'slicing' operation in ILWIS. The class 'non-vegetation' includes water bodies, rocky, sandy or barren land (Dupigny *et al.* 1999). Thus, the objective, delineation of water bodies from other land cover, is not served using NDVI classification. However, the areas under dense forest having high soil moisture are classified in the class 'vegetation'.

### Approach II: combinations of classified images

The combinations of different bands and classified images are used by many researchers for the detection and separation of various surface elements. Bhagat (2009) have combined classified NDVI and SWI raster images for the detection of potential areas of afforestation. Harma *et al.* (2001) have suggested band combinations for the interpretation of

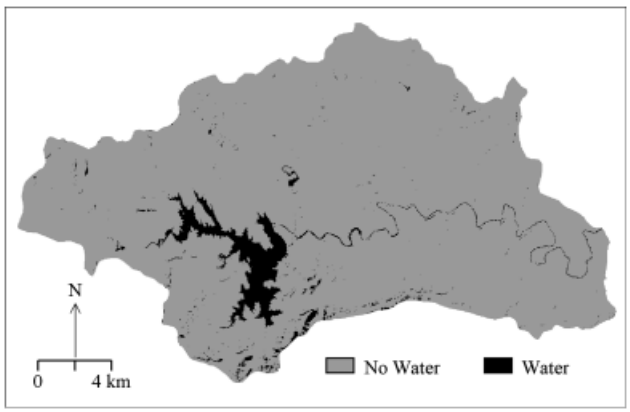


**Figure 3** | Distribution of water and non-water areas based on the SWI.

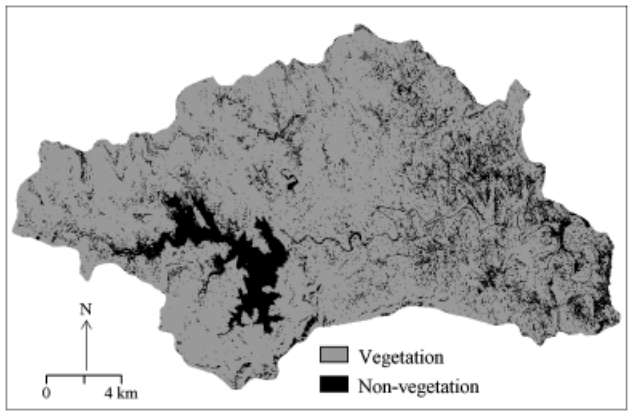


**Figure 4** | Distibution of vegetation and non-vegetation areas.

water quality. Here, the classified SWI raster image has been combined with a classified NDVI raster image for the detection of areas included in water bodies. The classes generated in this combination showing similar characteristics are merged using GIS software.

## Classified SWI and NDVI raster images

The combination (Figure 5) of classified SWI (Figure 3) and NDVI (Figure 4) raster maps prepared in 'approach I' has generated four classes (Table 1) such as (1) vegetation × water, (2) vegetation × no-water, (3) non-vegetation × water and (4) non-vegetation × no-water. Here, it is considered that dense vegetation cannot be grown in the temporary water bodies, especially in man-made reservoirs and flowing water. Therefore, out of these combinations, the class 'non-vegetation × water' is considered as a water body (Figure 5). The class 'vegetation × water' shows comparatively more surface wetness and dense vegetation. These areas have been detected and corrected from the class 'water' in the classification based on the SWI in the last approach. However, shadows associated with steep slopes are still included in this classified water body due to having the same reflectance (Frazier & Page 2000; Small 2004; Hendriks & Pellikka 2007).

**Table 1** | Class merging scheme

| | Vegetation classes | |
|---|---|---|
| **Wetness classes** | **Vegetation** | **Non-vegetation** |
| Water | Non-water (dense vegetation) | Water |
| No-water | Non-water (sparse vegetation) | Non-water (rocky, sandy and barren lands) |

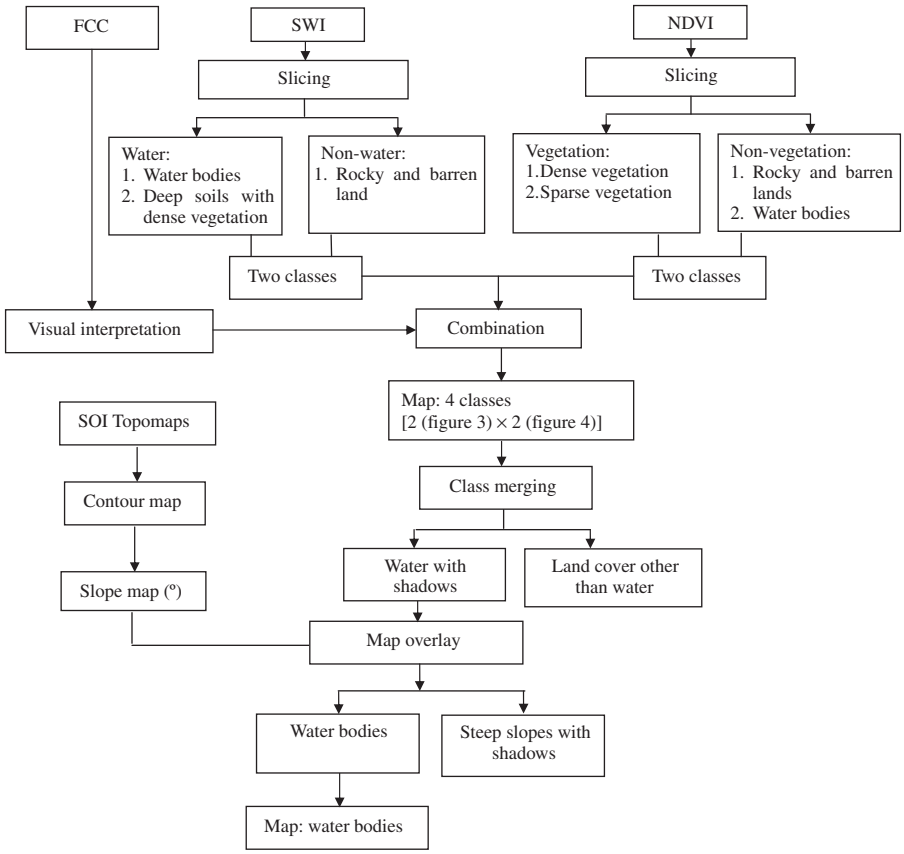


**Figure 5** | Schematic for image processing.

### Combined raster image (SWI and NDVI) and slope map

Fresh water and shadows appears similar in optical–infrared remote sensing data and cause confusion for image classification studies (Small 2004). There are two common causes of shadows, i.e. topographic features and clouds. The high lands or clouds block direct solar radiation from reaching the surface and being reflected to the sensor (Giles 2001; Bolch *et al.* 2008). Automated delineation of shadows included in the results after image processing remains a challenging task for the analysts (Racoviteanu *et al.* 2009). Visual interpretation and manual editing have been widely suggested for the correction of topographic shadowing effects. Digital terrain information generated in GIS was demonstrated to be useful for automated image analysis, data processing and modelling (Giles 2001; Bolch *et al.* 2008; Racoviteanu *et al.* 2009). The image used for the study is captured in cloudless clear weather. The shadows appearing in the image are only due to steep and high land topography. Therefore, they are detected and delineated in a combination of the combined raster image (classified SWI and NDVI) and the slope map.

The slope map has been prepared (Figure 2) using topomaps (Survey of India- 47E/10, 47E/11, 47E/14, 47E/15, surveyed in 1973–4). The contours (20 m interval) have been digitised using these topomaps and the slope is calculated in degrees using the operator 'slope – output slopemap in degree' available in the ILWIS (Academic 3.4) GIS software. The resolution of the calculated slope map is 28.5 m. The slope map has been classified into different broad classes (Table 2) using the 'slicing' operator. This classified slope map has been combined with the raster map showing water bodies (Figure 5) for the detection and correction of the area under shadows included in the class 'water'. Here, it is considered that water can be stored in gently sloping ($<1^{\circ}$) or flat areas. The shadows are associated with 'very steep (12–20°) to precipitous ($>30^{\circ}$) (Table 2) land in the study areas. Therefore, the area of shadows on 'very steep to precipitous' slopes included in the class 'water' was delineated from the water bodies by separating the areas of 'very steep to precipitous' slopes. The spatial query was performed using a simple overlay technique, i.e. logical operators for the delineation. Finally, water bodies in the form of reservoirs, small tanks built on small tributaries and some land covered by a thin water film due to springs have been detected.

**Table 2** | Slope classes

| No. | Class | Slope (°) | Area (ha) |
|---|---|---|---|
| 1 | Gentle | <1 | 2931 |
| 2 | Moderate | 1–3 | 4463 |
| 3 | Stiff | 3–6 | 5650 |
| 4 | Steep | 6–12 | 7765 |
| 5 | Very steep | 12–20 | 6270 |
| 6 | Extra steep | 20–30 | 4954 |
| 7 | Precipitous | >30 | 3759 |

## RESULTS AND DISCUSSION

### Approach I

### Distribution of water and non-water areas based on SWI

The surface wetness index estimated using at-satellite reflectance-based Tasselled Cap Coefficients suggested by Huang *et al.* (2002) is found to be more suitable than the NDVI to delineate the water bodies from other land cover (Figure 4). The area under 'water bodies' is estimated to be about 4.8% (1713 ha) of the total reviewed land (35 794 ha) and 95.2% under other land cover (Table 3). The water bodies includes major dams, small tanks built on small tributaries and springs in the foothill zones. However, the areas of high wetness in deep soils covered by dense deciduous and evergreen monsoon forest and shadows on sloping areas on northern hill sides are also included in the class 'water'. Also (1) all types of other forests, (2) rocky and barren land, and (3) sandy, rocky and barren areas in rivers and dams are included in the category 'non-water'. Thus, the estimated area of water bodies includes deep soils covered by dense forests and shadows which have to be separated.

**Table 3** | Distribution of water and non-water areas based on the SWI

| No. | Class | Threshold SWI | Area (ha) | Area (%) |
|---|---|---|---|---|
| 1 | Non-water | ≤2 | 34 081 | 95.2 |
| 2 | Water | ≥2 | 1713 | 4.8 |
| Total | | | 35 794 | 100 |

### Vegetation and non-vegetation areas

The pixels showing NDVI values in the raster image are clustered into two classes, i.e. 'vegetation' and 'non-vegetation'. About 82.8% of the study area (Table 4) is classified in the category 'vegetation' and 17.2% (29 654 ha) into 'non-vegetation'. The class 'vegetation' (Figure 4) includes all types of vegetation, i.e. dense forest, spares forest, bushes, crops and grass. Band 4 (IR) is highly sensitive to the chlorophyll content in plant leaves. The reflectance from freshwater bodies, and barren, rocky and metalled areas is recording the absence of plants and chlorophyll content. Therefore, all these kinds of areas without vegetation are accounted for in the class 'non-vegetation', i.e. water bodies, rocky, sandy and barren lands. The class 'vegetation' includes areas under dense vegetation on deep soil where soil moisture is high and included in the class 'water' found in the SWI classification.

## Approach II

### Estimated water bodies based on SWI and NDVI

About 4.5% (1595 ha) of the total reviewed area (Table 5) has been classified as water bodies in combined maps of classified SWI and NDVI classes (Figure 5). This figure is less (4.5%) than the water bodies estimated by using the SWI (4.8%). It means that about 0.3% (119 ha) of the area included in the SWI-based classification is detected and omitted in this approach. The deep-soil dense forested areas are separated by the combined process of classified SWI and NDVI raster images. However, the areas covered by shadows on very steep northern slopes are still included in this estimated area of water bodies (Figure 6).

### Detection and correction of shadows' effect

The assessment of the shadows' effect is omitted in the process of map combination, i.e. (1) water bodies with shadows (Figure 6) and (2) the distribution of slopes (Figure 2). The area under water bodies (Figure 7) is estimated as about 3.8% (1370 ha) of the total area reviewed in the present study (Table 6). About 0.7% (225 ha) of the total reviewed area is covered by topographic shadows, which are included in water bodies detected in the previous combination.

Thus, the area under 'water bodies' estimated using the SWI raster image accounts for about 4.8% (1713 ha) of the total reviewed area. About 20% of this classified area as water bodies has been detected as areas under dense vegetation (119 ha) and topographic shadows (343 ha). Finally, about 3.8% (1370 ha) of the total area reviewed is estimated as 'water bodies' in the study area. These water bodies include (1) the Wilson dam, (2) the Pravara River, (3) two small dams on small tributaries in the northern area, (4) springs in the foothill zones and (5) small dams on the minor streams. The springs and small dams are very much smaller in size than shown in the satellite window of the final resulting map (Figure 7).

**Table 4** | Distribution of vegetation and non-vegetation areas

| No. | Class | Threshold NDVI | Area (ha) | Area (%) |
|---|---|---|---|---|
| 1 | Non-vegetation | $\leq 0$ | 6140 | 17.2 |
| 2 | Vegetation | $\geq 0$ | 29654 | 82.8 |
| Total | | | 35794 | 100.0 |

**Table 5** | Estimated area under water bodies based on combination of SWI with NDVI

| No. | Class | Area (ha) | Area (%) |
|---|---|---|---|
| 1 | Non-water | 34 200 | 95.5 |
| 2 | Water | 1594 | 4.5 |
| Total | | 35 794 | 100.0 |

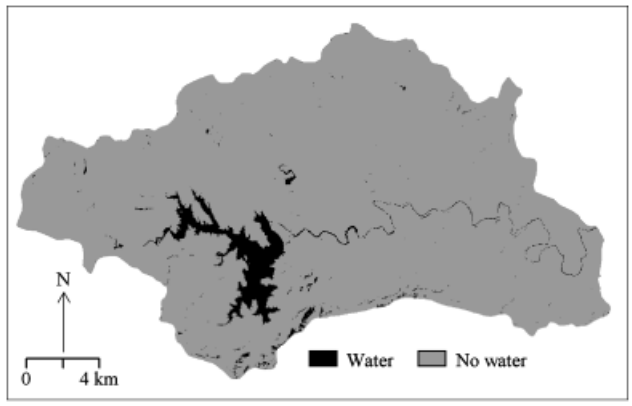


**Figure 6** | Estimated water bodies based on SWI and NDVI.

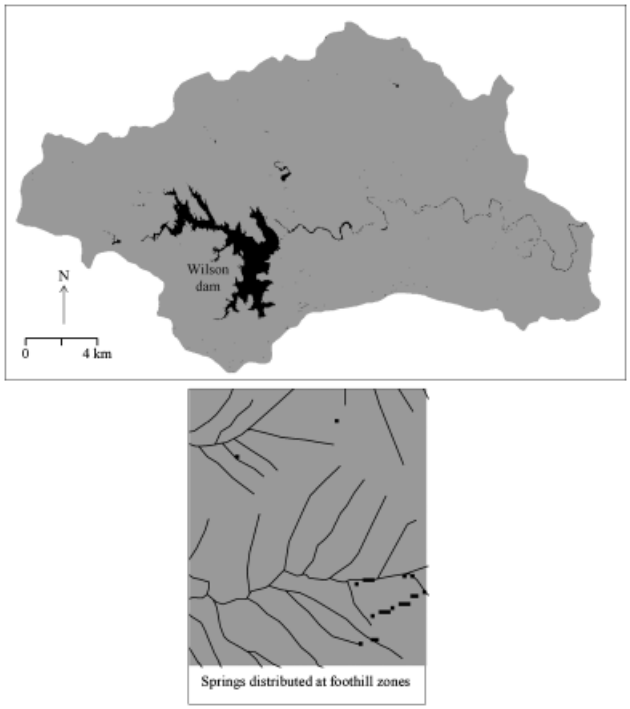


**Figure 7** | Distribution of water bodies.

**Table 6** | Distribution of water bodies

| No. | Class | Area (ha) | Area (%) |
|---|---|---|---|
| 1 | Non-water | 34 424 | 96.2 |
| 2 | Water | 1370 | 3.8 |
| Total | | 35 794 | 100.0 |

## ACCURACY ASSESSMENT

Accuracy assessment is a comparison between the classes obtained in the image processing and the reference classes for particular elements studied. Rahman & Saha (2008) have suggested that the sample size should take at least 30 samples for each category for an accuracy estimation of 90%. The reference data can be considered as the reference literature, i.e. maps, classified images, etc.. or data collected by offering 'ground validation'. In the present study, classification categories have been compared with the data obtained from ground validation and Google Earth images (124 samples) in the 'Error matrix' (Table 7) and accuracy estimated at the user's, producer's and overall accuracy level.

The overall accuracy of the classified final map is estimated at about 91.74% with variation in producer's and user's accuracy. The major water bodies are estimated up to 96.77% for the producer's and 100% for the user's accuracy. The assessment of the areas under shadows is omitted using simple topographic information in GIS. However, the slope map generated for the study has some errors in slope calculations. In the process of final combination, some areas under major water bodies at the border are omitted due to this miscalculated slope area. These incorrect digital calculations have reduced the accuracy of the classified map. The small rivers have less producer's (95.83%) and user's (92%) accuracy. The springs are more unstable, while thin and confused water bodies in nature are estimated at about 92.31% producer's and 85.71% user's accuracy. Some of the springs may become dry after the process of image capturing.

**Table 7** | Error matrix

| | Reference class | | | | | | |
|---|---|---|---|---|---|---|---|
| **Classified classes** | **Major dam** | **Minor tanks** | **River** | **Springs** | **Non-water lands** | **Total samples** | **User's accuracy (%)** |
| Major dam | **30** | 0 | 0 | 0 | 0 | 30 | **100** |
| Minor tanks | 0 | **11** | 0 | 0 | 0 | 11 | **100** |
| River | 0 | 0 | **23** | 0 | 2 | 25 | **92.00** |
| Springs | 0 | 0 | 0 | **24** | 4 | 28 | **85.71** |
| Non-water lands | 1 | 0 | 1 | 2 | **23** | 27 | **85.19** |
| Total samples | 31 | 11 | 24 | 26 | 29 | **121** | |
| **Producer's accuracy (%)** | **96.77** | **100** | **95.83** | **92.31** | **79.31** | **Overall accuracy 91.74%** | |

## CONCLUSIONS

The detection of water bodies provides the information base for better planning, managing and monitoring water resources. The remotely sensed Landsat ETM + dataset is useful for the detection and delineation of water bodies. The SWI generated using at-satellite reflectance based on Tasselled Cap Coefficients (Huang *et al.* 2002) is useful to get the combined effect of bands 1–5 and 7 in a single raster image which can be sliced into different classes. The SWI raster image is classified into classes 'water' and 'non-water'. The class 'water' is estimated as about 4.8% area of the total reviewed area. However, the class 'water' includes areas of deep soils covered by dense 'evergreen and deciduous' forest and areas under topographic shadows where the SWI values appeared high. Therefore, classified SWI and NDVI maps were combined together to detect and correct the assessment of areas under vegetation into water bodies. About 4.5% of the total reviewed area is detected as water bodies and 0.3% of the area under dense vegetation is included in the water bodies in SWI slicing.

Fresh water and shadows appear similar in optical–infrared remote sensing data. The shadows are included in water bodies estimated (4.5%) in the combined raster map using the SWI and NDVI, which need to be separated. The shadows appearing in the image data taken for the study are topographic in origin. Therefore, the raster map is combined with a slope map for the detection and correction of shadows from the water bodies. In this process, about 3.8% (1370 ha) of the total area reviewed is estimated as under water bodies and about 0.7% (225 ha) is covered by the topographic shadows.

The accuracy of the classified water bodies is improved by the process of multi-criteria analysis in approach II. About 1% of the reviewed area under vegetation (0.3%) and shadows (0.7%) included in water bodies estimated using the SWI is separated in this approach. The overall accuracy of the classified map is estimated as about 91.74% with 96.77% producer's and 100% user's accuracy for major water bodies in the study area. The relatively smaller water body objects, i.e. streams and springs, have less estimated producer's (92–96%) and user's (85–92%) accuracy.

The methodology formulated in this study may become an effective and rapid assessment tool prior to planning for available water resources in hilly zones, flood-affected and waterlogged areas based on previously acquired techniques for the identification of surface wetness levels and forest classifications using remotely sensed data and slope maps.

## ACKNOWLEDGEMENTS

The authors thanks ITC, The Netherlands for made available the GIS software (ILWIS 3.4) and the Global Land Cover Facility (GLCF), USA for providing the Landsat ETM + dataset free of charge. The University of Pune is thanked for funding support under research grants.

## REFERENCES

Bhagat, V. S. 2004 Utility status and trend of groundwater in the Purandhar tahsil of the Pune district. *Maharashtra. Uttar Pradesh Geogr. J.* **9**, 8–17.

Bhagat, V. S. 2008 Delineation of groundwater utility status areas using GIS techniques. *Enrich Environ. Multidisc. Int. Res. J.* **1**(3), 26–35.

Bhagat, V. S. 2009 Use of Landsat ETM + data for detection of potential areas for afforstation. *Int. J. Remote Sensing* **30**(10), 2607–2617.

Bindraban, P., Keulen, H. V. & Warner, F. J. 2006 Editorial. *Int. J. Wat. Res. Develop.* **22**(1), 1–2.

Bolch, T., Buchroithner, M. F., Peters, J., Baessler, M. & Bajracharya, S. 2008 Identification of glacier motion and potentially dangerous glacial lakes in the Mt. Everest region/Nepal using spaceborne imagery. *Natural Hazards Earth Syst. Sci.* **8**, 1329–1340.

Crist, E. P. 1985 A TM tasselled cap equivalent transformation for reflectance factor data. *Remote Sensing Environ.* **17**, 301–306.

Crist, E. P. & Cicone, R. C. 1984 A physically based transformation to thematic mapper data – the TM Tasselled cap. *IEEE Trans. Geosci. Remote Sensing* **22**, 256–263.

Crist, E. P., Laurin, R. & Ciocone, R. C. 1986 Vegetation and soil information contained in transformed Thematic Mapper data. In: *Proc. IGARSS Symposium* pp. 1465–1470. Available at: http://www.ciesin.org/docs/055-419.html. European Space Agency, Paris.

Dam van, J. C., Singh, R., Bessembinder, J. J. E., Lwffelaar, P. A., Bastiaanssen, W. G. M., Lhorar, R. K., Kroes, J. G. & Droogers, P. 2006 Assessing option to increase water productivity in irrigated river basin using remote sensing and modelling tools. *Wat. Res. Develop.* **22**(1), 115–133.

Dayaker, P. T. K. 2003 Mapping of potential fishing zones using OCM Data of Irs-P4 and geographic information system. *Environ. Informatics Arch.* **1**, 475–480.

Deosthali, V. 2005 *Prioritization of Villages for Reclamation of Salt-affected Areas in Irrigated tracts of Sangli District (M.S.): a GIS and Remote Sensing Approach*. Technical Report- GR 01/05, Department of Geography, University of Pune.

Dupigny, G., Lesley, A. & Lewis, J. E. 1999 A moisture index for surface characterization over a semi arid area. *Photogramm. Engng. Remote Sensing* **65**(8), 937–945.

Frazier, P. S. & Page, K. J. 2000 Water body detection and delineation with Landsat TM data. *Photogramm. Engng. Remote Sensing* **66**(12), 1461–1467.

Giles, P. T. 2001 Remote sensing and cast shadows in mountainous terrain. *Photogramm. Engng. Remote Sensing* **67**(7), 833–839.

Gong, P., Miao, X., Tate, K., Battaglia, C. & Biging, G. S. 2004 Water table level in relation to EO-1 AL.I and ETM+ data over a mountainous meadow in California. *Can. J. Remote Sensing* **30**(5), 691–696.

Harma, P., Vepsalainen, J., Hannonen, T., Pyhalahti, T., Kamari, J., Kallio, K., Eloheimo, K. & Koponen, S. 2001 Detection of water quality using simulated satellite data and semi-empirical algorithms in Finland. *Sci. Total Environ.* **268**(1–3), 107–121.

Hendriks, J. P. M. & Pellikka, P. 2007 Semi-automatic glacier delineation from Landsat imagery over Hintereisferner in the Austrian Alps. *Z. Gletscherkunde Undglazialgeologie* **41**, 55–75.

Huang, C., Wylie, B., Yang, L., Homer, C. & Zylstra, G. 2002 Derivation of a Tasselled cap transformation based on Landsat 7 at-satellite reflectance. *Int. J. Remote Sensing* **23**(8), 1741–1748.

Hui, F., Xu, B., Huang, H., Yu, Q. & Ggong, P. 2008 Modelling spatial-temporal change of Poyang Lake using multitemporal Landsat imagery. *Int. J. Remote Sensing* **29**(20), 5767–5784.

ILWIS 2004 *Windows-based, Integrated GIS and Remote Sensing Application*. Open source software. International Institute for Geo-Information Science and Earth Observation (ITC), Enschede, The Netherlands. Available at http://www.52north.org/.

Jongman, R. H. G. & Padovani, C. R. 2006 Interaction between stakeholders and researchers for integrated river basin management. *Wat. Res. Develop.* **22**(1), 49–60.

Kiage, L. M., Liu, K. B., Walker, N. D., Lam, N. & Huh, O. K. 2007 Recent land-cover/use change associated with land degradation in the Lake Baringo catchment, Kenya, East Africa: evidence from Landsat TM and ETM+. *Int. J. Remote Sensing* **28**(19), 1–25.

Kumar, S., Shirke, K. D. & Pawar, N. J. 2007 GIS-based colour composites and overlays to delineate heavy metal contamination zones in the shallow alluvial aquifers, Ankaleshwar Industrial Estate, South Gujarat, India. *Environ. Geol.* **54**(1), 117–129.

Mioc, D., Nickerson, B., MacGillivray, E., Mortonc, A., Anton, F., Fraser, D., Tang, P. & Liang, G. 2008 Early Warning and Mapping for Flood Disasters. In: *The International Archives of the Photogrammetry, Remote Sensing and Spatial Information Sciences* Vol. 37, Part B4. Reed Business, Lemmer, The Netherlands, pp. 1507–1512.

Oza, S. R., Singh, R. P., Dadhwal, V. K. & Desai, P. S. 2006 Large area soil moisture estimation and mapping using space-borne multi-frequency passive microwave data. *Photonirvachak. J. Ind. Soc. Remote Sensing* **34**(4), 343–350.

Patel, N. R. 2006 Modeling of wheat yields using multi-temporal Terra/MODIS satellite data. *Geocarto Int.* **21**(1), 43–50.

Pavlov, S. S., Roerink, G. J., Hellegers, P. J. G. J. & Popovych, V. F. 2006 Irrigation performance assessment in Crimea, Ukraine. *Wat. Res. Develop.* **22**(1), 61–78.

Pawar, N. J., Pawar, J. B., Kumar, S. & Supekar, A. 2008 Geochemical eccentricity of ground water allied to weathering of basalts from the Deccan Volcanic Province, India: insinuation on $CO_2$ consumption. *Aquat. Geochem.* **14**, 41–71.

Racoviteanu, A. E., Paul, F., Raup, B., Khalsa, S., Jodha, S. & Armstrong, R. 2009 Challenges and recommendations in mapping of glacier parameters from space: results of the 2008 Global Land Ice Measurements from Space (GLIMS) workshop, Boulder, CO, USA. *Annal. Glaciol.* **53**, 53–69.

Rahman, R. & Saha, S. K. 2008 Multi-resolution segmentation for object-based classification and accuracy assessment of land use/land cover classification using remotely sensed data. *Photonirvachak. J. Ind. Soc. Remote Sensing* **36**(2), 189–201.

Ramsey, R., Douglas, W., Dennis, L. & Mcginity, C. 2004 Evaluating the use of Landsat 30 m Enhanced Thematic Mapper to monitor vegetation cover in shrub-steppe environments. *Geocarto Int.* **19**(2), 39–47.

Ryu, J.- H., Won, J.- S., Min, K. D. 2002 Waterline extraction from Landsat TM data in a tidal flat: a case study in Gomso Bay, Korea. *Remote Sensing Environ.* **83**, 442–456.

Sanyal, J. & Lu, X. X. 2004 Application of remote sensing in flood management with special reference to monsoon Asia: a review. *Natural Hazards* **33**, 283–301.

Small, C. 2004 The Landsat ETM+ spectral mixing space. *Remote Sensing Environ.* **93**, 1–17.

Troell, J., Breuch, C., Cassar, A. & Schang, S. 2005 *Transboundary Environmental Impact Assessment as a Tool for Promoting Public Participation in International Watercourse Management, Enhancing Participation and Governances in Water Resource Management: Conventional Approaches and Information Technology*. United Nations University, Tokyo pp. 53–80.

Wang, G., Wente, S., Gertner, G. Z. & Anderson, A. 2002 Improvement in mapping vegetation cover factor for the universal soil loss equation by geostatistical methods with Landsat Thematic Mapper images. *Int. J. Remote Sensing* **23**(18), 3649–3667.

Warner, J. F., Bindraban, P. S. & Keulen, H. V. 2006 Introduction: water for food and ecosystem: how to cut which pie? *Wat. Res. Develop.* **22**(1), 3–13.

WHO (World Health Organization) 2003 *Water Sanitation and Health*. Available at: http://www.who.int/water_sanitation_helth/hygiene/en/ (accessed 24 March 2009).

WRI (World Resource Institute) 2004 *Water Resource eAtlas. Watersheds of the World. AS19 Mekong*. Available at: http://multimedia.wri.org/watersheds_2003/ (accessed 24 March 2009).

Wu, G. G., Leeuw, J. D., Skidmore, A. K., Prins, H. H. T. & Liu, Y. 2008 Comparison of MODIS and Landsat TM5 images for mapping tempo–spatial dynamics of Secchi disk depths in Poyang Lake National Nature Reserve, China. *Int. J. Remote Sensing* **29**(8), 2183–2198.

First received 20 January 2010; accepted in revised form 21 June 2010. Available online 22 November 2010